# An Integrated Approach to the Analysis and Design of a Three-Axis Cross-Coupling Control System

**Sungchul Jee[1,#] and Hakchul Lee[1]**

1 Department of Mechanical Engineering, Dankook University, Seoul, South Korea
# Corresponding Author / E-mail: scjee@dku.edu; TEL: +82-2-709-2911; FAX: +82-2-709-2569

KEYWORDS: Multi-axis CNC, Tracking, Axial controller, Contouring, Cross-coupling controller, Integrated controller design

*We propose a controller design analysis for a cross-coupling control system, which is essential for achieving high contouring accuracy in multi-axis CNC systems. The proposed analysis combines three axial controllers for each individual feed drive system together with a cross-coupling controller at the beginning of the design stage in an integrated manner. These two types of controllers used to be separately designed and analyzed since they have different control objectives. The proposed scheme is based on a mathematical formulation of a three-dimensional contour error model and includes a stability analysis for the overall control system and a performance analysis in terms of contouring and tracking accuracy at steady state. A computer simulation was used to demonstrate the validity of the proposed methodology. The performance variation was investigated under different operating conditions and controller gains, and a design range was elicited that met the given performance specifications. The results provide basic guidelines in systematic and comprehensive controller designs for multi-axis CNC systems. A cross-coupling control system was also implemented on a PC-based three-axis CNC testbed, and the experimental results confirmed the usefulness of the proposed control system in terms of contouring accuracy.*

Manuscript received: May 1, 2006 / Accepted: December 11, 2006

## 1. Introduction

Servo controllers for CNC machine tools can be classified as axial or cross-coupling. Axial controllers are intended to maximize the position tracking performance of individually driven axes for a given feedrate, and cross-coupling controllers[1-3] are used to improve the contouring performance by coordinating all the driven axes simultaneously based on contour error observations. These two types of controllers have different control objectives and are typically studied separately. Cross-coupling controllers have simply been added to axial controller platforms without considering the interactions between the two types of controllers, and research has focused mainly on verifying their performance. To improve the contouring accuracy of multi-axis CNC systems, cross-coupling controllers are essential and an integrated control system design is needed at the beginning of the design stage when both the contouring and tracking performance are considered. This paper proposes an integrated analysis methodology for a three-axis cross-coupling control system and provides basic guidelines for a design to improve the performance of multi-axis CNCs. A cross-coupling control system was also implemented on a PC-based three-axis CNC testbed, and the experimental results confirmed the utility of the proposed control system in terms of contouring accuracy.

## 2. Design Analysis of a Three-Axis Cross-Coupling Control System

### 2.1 Analysis of the contour error model

The relationship between the contour and tracking errors of a three-axis cross-coupling control system was examined using the approximations obtained from a nonlinear contour error model as functions of the tracking error. This provides a framework for further analysis and design of the control system. The three-dimensional

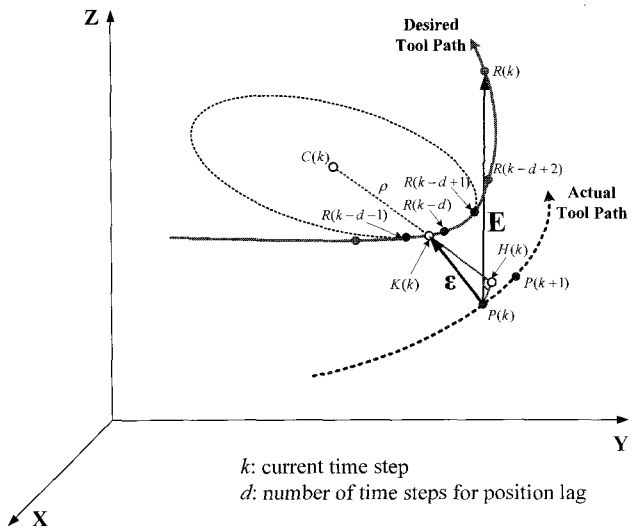


*k*: current time step
*d*: number of time steps for position lag

Fig. 1 Three-dimensional real-time contour error model

real-time contour error model[1] considered in this study utilized three neighboring reference points, $R(k-d-1)$, $R(k-d)$, and $R(k-d+1)$, in addition to the current actual position $P(k)$, as illustrated in Fig. 1, where $R(k-d)$ is the closest point to $P(k)$.

In the contour error approximation, for the sake of convenience, the contour error vector ε was projected onto two of the XY, YZ, and ZX planes, and each axial component of the contour error was derived for the analysis. The contour error vector projected on the XY plane, for example, can reflect the three-dimensional components $\varepsilon_x$ and $\varepsilon_y$. Using the approximation $K(k) \approx R(k-d)$, where $K(k)$ is the intersection of $CH$ with the circle created by the three reference points, the contour error vector projected on the XY plane can be defined by

$$\boldsymbol{\varepsilon}_1 = \boldsymbol{\varepsilon}' + \boldsymbol{\varepsilon}'' \tag{1}$$

as shown in Fig. 2. Therefore, by representing the vectors $\boldsymbol{\varepsilon}'$ and $\boldsymbol{\varepsilon}''$ with the geometric angles shown in Fig. 2 and the tracking error, we can obtain the relationship between the contour and tracking errors.

Using a Taylor series expansion of point $Q(k)$ with respect to point $R(k-d)$ and the geometry shown in Fig. 2, we can derive the axial components of $\varepsilon_1$, after some mathematical manipulations, as

$$\varepsilon_x = (C_1 \cos\nu_1)E_x + (C_1 \sin\nu_1)E_y = A_{1x}E_x + A_{1y}E_y \tag{2}$$
$$\varepsilon_y = (C_2 \cos\nu_1)E_x + (C_2 \sin\nu_1)E_y = B_{1x}E_x + B_{1y}E_y \tag{3}$$

where

$$C_1 = \frac{1}{C_5}(C_3\cos\nu_1 + C_4\sin\nu_1)(-\sin\varphi_1) + \left(\frac{1}{C_5} - 1\right)\cos\nu_1$$
$$\approx (C_3\cos\nu_1 + C_4\sin\nu_1)(-\sin\varphi_1)$$
$$C_2 = \frac{1}{C_5}(C_3\cos\nu_1 + C_4\sin\nu_1)\cos\varphi_1 + \left(\frac{1}{C_5} - 1\right)\sin\nu_1$$
$$\approx (C_3\cos\nu_1 + C_4\sin\nu_1)\cos\varphi_1$$
$$C_3 = -\sin\varphi_1 - \frac{\cos(\varphi_1 - \nu_1)}{\sin\omega_1}\cos\nu_1\cos\omega_1$$
$$C_4 = \cos\varphi_1 - \frac{\cos(\varphi_1 - \nu_1)}{\sin\omega_1}\sin\nu_1\cos\omega_1$$
$$C_5 = \frac{\sqrt{1-\cos^2(\omega_1 + \delta_1 - \varphi_1)}}{\cos(\delta_1 - \nu_1)\sin\omega_1}\cos(\varphi_1 - \nu_1) \approx 1$$
$$A_{1x} = C_1\cos\nu_1\ ;\ A_{1y} = C_1\sin\nu_1$$
$$B_{1x} = C_2\cos\nu_1\ ;\ B_{1y} = C_2\sin\nu_1$$

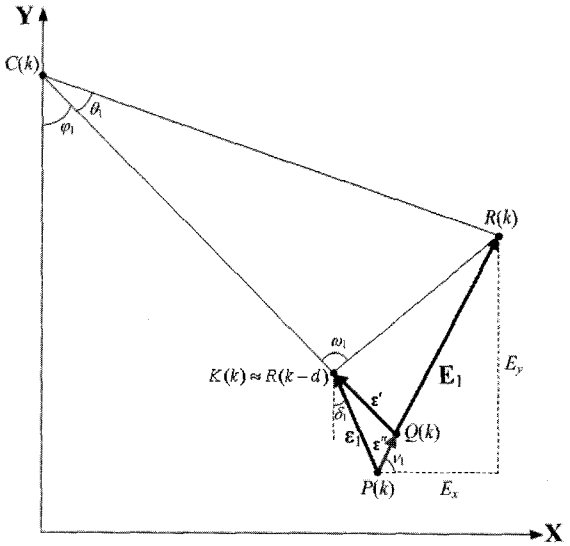


Fig. 2 Contour error vector projected onto the XY plane

Hence, as shown by Eqs. (2) and (3), it is possible to define the contour error components along the X- and Y-axes using a combination of geometric angles and the tracking error components. Similarly, the contour error components on the YZ plane are as follows:

$$\varepsilon_y = (D_1\cos\nu_2)E_y + (D_1\sin\nu_2)E_z = B_{2y}E_y + B_{2z}E_z \tag{4}$$
$$\varepsilon_z = (D_2\cos\nu_2)E_y + (D_2\sin\nu_2)E_z = C_{2y}E_y + C_{2z}E_z \tag{5}$$

where $\nu_2 = \tan^{-1}(E_z / E_y)$, and $D_1$ and $D_2$ are defined using the angles on the YZ plane in the same manner as $C_1$ and $C_2$. Likewise, the following relations are obtained for the ZX plane:

$$\varepsilon_z = C_{3z}E_z + C_{3x}E_x \tag{6}$$
$$\varepsilon_x = A_{3z}E_z + A_{3x}E_x \tag{7}$$

Consequently, the three-dimensional contour error can be expressed as a function of the tracking error, which facilitates various analyses in the succeeding design process.

### 2.2 Stability analysis of the cross-coupling control system

A stability analysis was performed for the three-axis cross-coupling control system shown in Fig. 3, in which a proportional controller and a PID controller were employed for individual axis control and cross-coupling control, respectively. Let the diagonal matrix be $\mathbf{K}_P$, whose diagonal elements are the proportional gains $K_{Pi}$ ($i$ = $x$, $y$, $z$) of each axial controller. Also let the cross-coupling controller matrix be $\mathbf{G}_C$ (= $G_C\mathbf{I}$), where

$$G_C(z) = C_P + C_I\frac{Tz}{z-1} + C_D\frac{z-1}{Tz} \tag{8}$$

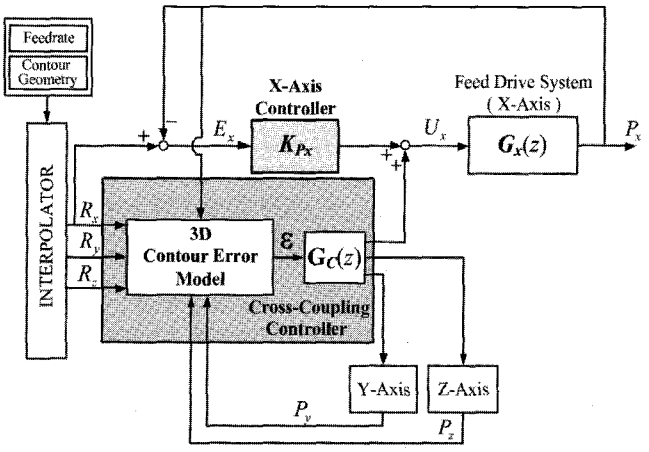


Fig. 3 Three-axis cross-coupling control system

If we let the transfer function matrix for the feed drive system be $\mathbf{G}(z)$, then its diagonal elements are defined as follows with open-loop gains $K_i$ and time constants $\tau_i$ for each axis and sampling period $T$:

$$G_i(z) = \frac{H_{1i}z + H_{0i}}{(z-1)(z-r_i)} \quad (i = x, y, z) \tag{9}$$

where

$$H_{1i} = K_i(T - \tau_i + \tau_i r_i)$$
$$H_{0i} = K_i(\tau_i - \tau_i r_i - Tr_i)$$
$$r_i = \exp(-T/\tau_i)$$

In the above case, the position output vector $\mathbf{P}(z)$ and the control signal vector $\mathbf{U}(z)$ are given by

$$\mathbf{P}(z) = \mathbf{G}(z)\mathbf{U}(z) \tag{10}$$
$$\mathbf{U}(z) = \mathbf{K}_P\mathbf{E}(z) + \mathbf{G}_C\boldsymbol{\varepsilon}(z) \tag{11}$$

Since each axial component $\varepsilon_i$ of the contour error was defined as a combination of tracking error components on the projected plane,

Eq. (11) can be expressed as

$$\mathbf{U}(z)=[\mathbf{K_P}+\mathbf{G_C}(z)\mathbf{M}(z)]\mathbf{E}(z)\equiv\mathbf{T}(z)\mathbf{E}(z) \tag{12}$$

In Eq. (12), $\mathbf{M}(z)$ corresponds to a transformation matrix between $\boldsymbol{\varepsilon}(z)$ and $\mathbf{E}(z)$. From Eqs. (2) through (7), $\mathbf{M}(z)$ can be defined as

$$\mathbf{M}(z)=\frac{1}{2}\begin{bmatrix} A_{1x}+A_{3x} & A_{1y} & A_{3z} \\ B_{1x} & B_{1y}+B_{2y} & B_{2z} \\ C_{3x} & C_{2y} & C_{2z}+C_{3z} \end{bmatrix} \tag{13}$$

In Eq. (13), subscripts 1, 2, and 3 indicate that the coefficients are defined on the XY, YZ, and ZX planes, respectively. Combining Eqs. (10) and (12), we obtain a relationship between the position error and the position output vector,

$$\mathbf{P}(z)=\mathbf{G}(z)\mathbf{T}(z)\mathbf{E}(z)\equiv\boldsymbol{\Omega}(z)\mathbf{E}(z) \tag{14}$$

For the sake of convenience, Eq. (14) is decomposed into XY and YZ (or ZX) planes. By applying Eq. (14) to the characteristic equation for each plane,

$$\det\left|\mathbf{I}+\boldsymbol{\Omega}_{ij}(z)\right|=0 \tag{15}$$

a stability analysis for the overall system can be performed. In Eq. (15), the subscript $ij$ represents the projected plane.

In our stability analysis, we first assumed a matched system, in which the X-, Y-, and Z-axes have the same system parameters, $H_{1i}=H_1$, $H_{0i}=H_0$, and $r_i = r$ in Eq. (9) and the position feedback controller gains $K_{Pi}=K_P$, which makes Eq. (15) appear as

$$\Omega_1(z)\Omega_2(z)=0 \tag{16}$$

where

$\Omega_1(z)=(z-1)(z-r)+K_P(H_1z+H_0)$
$\Omega_2(z)=(z-1)(z-r)+[K_P+G_C(z)M](H_1z+H_0)$
$M=A_{1x}+B_{1y}$ (XY plane) or $B_{2y}+C_{2z}$ (YZ plane)

By applying Jury's stability criterion to each system defined on the projected plane and performing the stability analysis repeatedly for each different set of (*i.e.*, mismatched) feed drive system parameters, a common stability range of the controller gains can be determined for the overall three-axis system.

As a result, from the conditions on $\Omega_1(z)$, a stable range for the position feedback controller gain is acquired from

$$K_P<\min_{i=x,y,z}[(1-r_i)/H_{0i}] \tag{17}$$

Then, by reflecting the above inequality in the conditions on $\Omega_2(z)$, stable ranges for the cross-coupling controller gains $C_P$, $C_I$, and $C_D$ can be obtained. In the meantime, the coefficient $M$ is intricately defined using the angles given in Section 2.1. It is necessary to first determine its possible range using a computer program and inject this into the stability conditions such that the stable ranges for the controller gains are minimized.

### 2.3 Performance analysis of the cross-coupling control system

For the system shown in Fig. 3, a performance analysis was conducted for three-dimensional circular motion from two different points of view: contouring and tracking. In this analysis, we assumed a matched three-axis system.

The contour and tracking error vectors were defined for a reference position input vector $\mathbf{R}(z)$ as

$$\boldsymbol{\varepsilon}(z)=z^{-d}\mathbf{R}(z)-\mathbf{P}(z) \tag{18}$$
$$\mathbf{E}(z)=\mathbf{R}(z)-\mathbf{P}(z) \tag{19}$$

In Eq. (18), $d$ indicates the number of time steps for the position lag. From Eqs. (10), (11), (18), and (19), the following relationships can be deduced:

$$\mathbf{P}(z)=\mathbf{H}(z)\mathbf{R}(z) \tag{20}$$
$$\mathbf{H}(z)\equiv[\mathbf{I}+\mathbf{G}(z)\{\mathbf{K_P}+\mathbf{G_C}(z)\}]^{-1}\mathbf{G}(z)[\mathbf{K_P}+z^{-d}\mathbf{G_C}(z)] \tag{21}$$

In the case of three-dimensional circular motion, the reference input vector can be expressed by

$$\mathbf{R}(z)=R_0\mathbf{u}C(z)+R_0\mathbf{v}S(z) \tag{22}$$

where $R_0$ is the radius of a circle, $\mathbf{u}$ and $\mathbf{v}$ are the orthonormal basis for the circle, and $C(z)$ and $S(z)$ are the z-transform of cos $\omega kT$ and sin $\omega kT$, respectively ($\omega$: reference angular velocity). Accordingly, based on Eqs. (20) and (22), the position output vector can be rearranged as

$$\mathbf{P}(z)=\mathbf{U_H}(z)C(z)+\mathbf{V_H}(z)S(z) \tag{23}$$

where $\mathbf{U_H}(z)=R_o\mathbf{H}(z)\mathbf{u}$ and $\mathbf{V_H}(z)=R_o\mathbf{H}(z)\mathbf{v}$. To obtain a discrete-time response of Eq. (23), we define

$$\mathbf{L}(e^{j\omega T})=\mathbf{U_H}(e^{j\omega T})-j\mathbf{V_H}(e^{j\omega T})=\mathbf{a}+j\mathbf{b} \tag{24}$$

Then the real vectors $\mathbf{a}$ and $\mathbf{b}$ are as follows:

$$\mathbf{a}=\mathrm{Re}\{\mathbf{L}(e^{j\omega T})\} \tag{25}$$
$$\mathbf{b}=\mathrm{Im}\{\mathbf{L}(e^{j\omega T})\} \tag{26}$$

and the steady-state response of the position output can be obtained from

$$\mathbf{P}(kT)=\mathrm{Re}\{\mathbf{L}(e^{j\omega T})e^{j\omega kT}\}=\mathbf{a}\cos\omega kT-\mathbf{b}\sin\omega kT \tag{27}$$

The magnitude of the contour error for three-dimensional circular motion can be defined as

$$\begin{aligned}\varepsilon&=\|\boldsymbol{\varepsilon}\|=(\mathbf{P}^{\mathrm{T}}\mathbf{P})^{1/2}-R_0\\&=\left[\begin{array}{c}\frac{1}{2}\left(\|\mathbf{a}\|^2+\|\mathbf{b}\|^2\right)+\frac{1}{2}\left(\|\mathbf{a}\|^2-\|\mathbf{b}\|^2\right)\cos 2\omega kT\\-\mathbf{a}^{\mathrm{T}}\mathbf{b}\sin 2\omega kT\end{array}\right]^{1/2}-R_0\end{aligned} \tag{28}$$

In Eqs. (25) and (26), if the three axes are matched, $\|\mathbf{a}\|=\|\mathbf{b}\|$ and $\mathbf{a}^{\mathrm{T}}\mathbf{b}=0$, the magnitude of the contour error is given by

$$\varepsilon=\|\mathbf{a}\|-R_0=\left\|\mathrm{Re}\{\mathbf{L}(e^{j\omega T})\}\right\|-R_0 \tag{29}$$

From Eqs. (19) and (20), the tracking error vector for the reference position input vector can be represented as

$$\mathbf{E}(z)=[\mathbf{I}-\mathbf{H}(z)]\mathbf{R}(z)\equiv\mathbf{J}(z)\mathbf{R}(z) \tag{30}$$

By substituting Eq. (22) into Eq. (30) and following the same procedure as that for the position output response, we can obtain the magnitude of the tracking error at steady state:

$$E=\|\mathbf{E}\|=(\mathbf{E}^{\mathrm{T}}\mathbf{E})^{1/2}=R_0\left\|\mathrm{Re}\{\mathbf{J}(e^{j\omega T})\mathbf{u}-j\mathbf{J}(e^{j\omega T})\mathbf{v}\}\right\| \tag{31}$$

The values of the above equations are all determined by the unknown constant $d$. This constant can be numerically calculated such that it simultaneously satisfies Eqs. (18), (27), and

$$\boldsymbol{\varepsilon}(kT)^{\mathrm{T}}\dot{\mathbf{R}}((k-d)T)=0 \tag{32}$$

which indicates that the contour error vector is normal to the velocity vector at point $R(k-d)$. Consequently, it is possible to predict the

contouring and tracking performance accurately at steady state for the three-axis control system according to the operating conditions (*i.e.*, the feedrate and radius of curvature of a contour) and controller gains, which can be applied to the controller design considering both performance together in an integrated manner.

## 3. Simulation and Experimental Results

To verify the validity of the proposed stability analysis for the system described in Table 1, the results were compared with those obtained from a separate computer simulation shown in Fig. 4, where $0 < K_P < 16.64$. The figure indicates that the proposed analysis is appropriate for this system.

Table 1 System parameters

| Parameters | X-axis | Y-axis | Z-axis |
|---|---|---|---|
| Open-loop gain ($s^{-1}$) | 121 | 118 | 83 |
| Time constant (s) | 0.025 | 0.03 | 0.01 |
| Basic length unit (BLU) | 0.5 μm | | |
| Sampling time (s) | 0.001 | | |

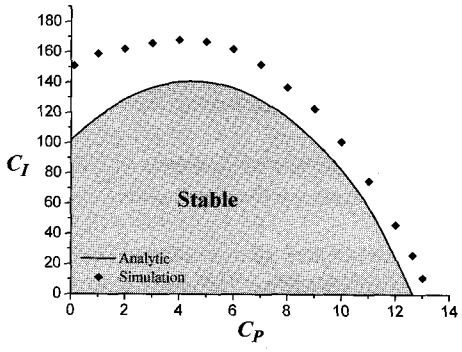


Fig. 4(a) Stability range for controller gains $C_P$ and $C_I$

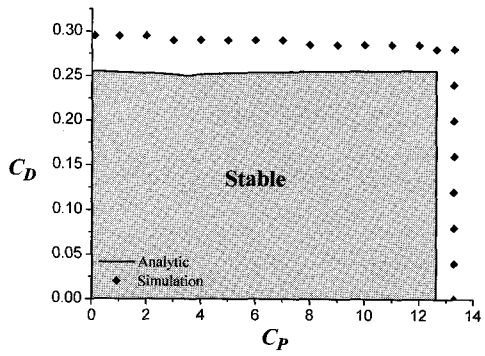


Fig. 4(b) Stability range for controller gains $C_P$ and $C_D$

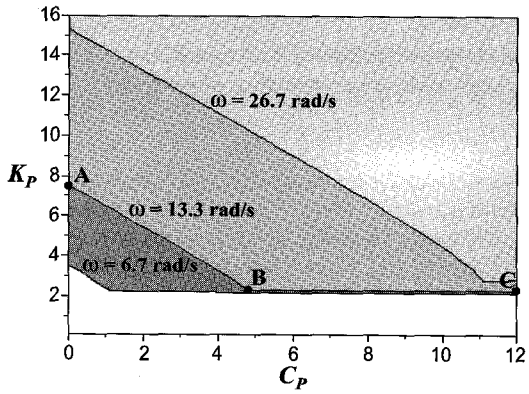


Fig. 5 Design range of the controller gains for different input frequencies

From the performance analysis, an example range of controller gains that satisfies both a contouring accuracy of 25 μm and a tracking accuracy of 250 μm is illustrated in Fig. 5 for three reference angular velocities. In this example, we assumed that $C_I = 2.62C_P$ and $C_D = 0.02C_P$. We considered a suitable proportional gain $C_P$ of the cross-coupling controller to be one that maximizes the contouring performance for the feedback controller gain $K_P$ chosen such that the tracking performance is restricted to the required minimum because the tracking performance is not critical to the machining accuracy. In this context, a suitable set of gains for the given operating conditions can be found in the lower right portion of the design range (*i.e.*, in the vicinity of point C) in Fig. 5. The simulation results shown in Fig. 6 validate this principle used to determine the controller gains.

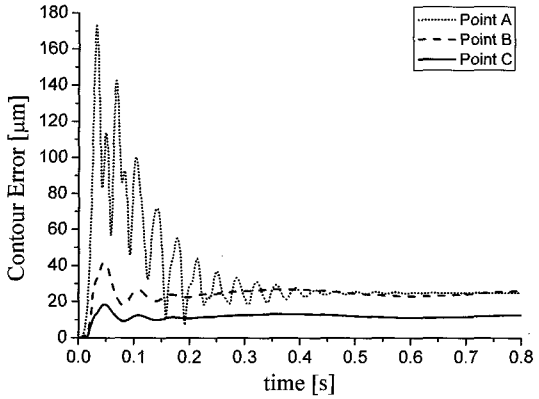


Fig. 6 Simulation results of the contour errors at selected points in the design range

To evaluate the actual performance of the proposed three-axis cross-coupling control system, we implemented it on a PC-based three-axis CNC testbed that had a position resolution of 0.153 μm. The actual contour error of the control system is shown in Fig. 7 for three-dimensional circular motion with a radius of 50 mm and a high feedrate of 10 m/min. This result confirms the utility of the proposed control system in terms of contouring accuracy.

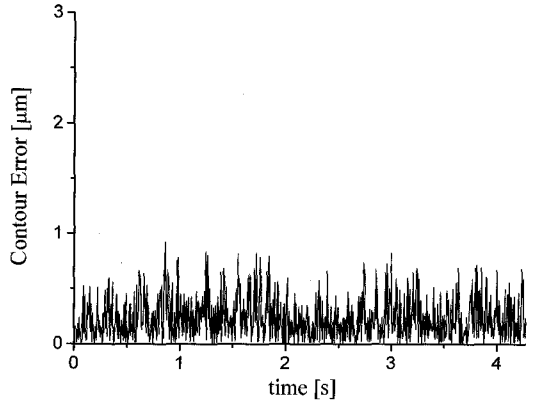


Fig. 7 Experimental contouring accuracy obtained using the proposed cross-coupling control system

## 4. Conclusions

We proposed a stability analysis method for a three-axis cross-coupling control system based on a mathematical analysis of a three-dimensional contour error model, and also a methodology for a performance analysis that can accurately determine the contouring and tracking performance at steady state for matched systems. We verified the proposed approaches through computer simulations and validated the utility of the proposed control system in terms of contouring accuracy by performing an actual experiment.

## ACKNOWLEDGEMENT

This research was supported by a grant from the Materials & Components Technology R&D Program funded by the Ministry of Commerce, Industry and Energy, Republic of Korea.

## REFERENCES

1. Koren, Y. and Lo, C. C., "Variable-Gain Cross-Coupling Controller for Contouring," Annals of the CIRP, Vol. 40, No. 1, pp. 371–374, 1991.
2. Yeh, S. S. and Hsu, P. L., "Analysis and Design of Integrated Control for Multi-Axis Motion Systems," IEEE Transactions on Control Systems Technology, Vol. 11, No. 3, pp. 375–382, 2003.
3. Jee, S. and Koo, T., "3-Axis Coupling Controller for High-Precision/High-Speed Contour Machining," Transactions of the KSME, A, Vol. 28, No. 1, pp. 40–47, 2004.